HHS Public Access

Author manuscript

J Vis Exp. Author manuscript; available in PMC 2020 June 01.

Real-time In Vitro Monitoring of Odorant Receptor Activation by an Odorant in the Vapor Phase

Claire A. de March[1], **Yosuke Fukutani**[1,2], **Aashutosh Vihani**[1,3], **Hitoshi Kida**[1,4], **Hiroaki Matsunami**[1,3,5,6]

[1]Department of Molecular Genetics and Microbiology, Duke University Medical Center

[2]Department of Biotechnology and Life Science, Tokyo University of Agriculture and Technology

[3]Department of Neurobiology, Duke University Medical Center

[4]Department of Mechanical Systems, Engineering, Tokyo University of Agriculture and Technology

[5]Institute of Global Innovation Research, Tokyo University of Agriculture and Technology

[6]Duke Institute for Brain Sciences, Duke University

Abstract

Olfactory perception begins with the interaction of odorants with odorant receptors (OR) expressed by olfactory sensory neurons (OSN). Odor recognition follows a combinatorial coding scheme, where one OR can be activated by a set of odorants and one odorant can activate a combination of ORs. Through such combinatorial coding, organisms can detect and discriminate between a myriad of volatile odor molecules. Thus, an odor at a given concentration can be described by an activation pattern of ORs, which is specific to each odor. In that sense, cracking the mechanisms that the brain uses to perceive odor requires the understanding odorant-OR interactions. This is why the olfaction community is committed to “de-orphanize” these receptors. Conventional in vitro systems used to identify odorant-OR interactions have utilized incubating cell media with odorant, which is distinct from the natural detection of odors via vapor odorants dissolution into nasal mucosa before interacting with ORs. Here, we describe a new method that allows for real-time monitoring of OR activation via vapor-phase odorants. Our method relies on measuring cAMP release by luminescence using the Glosensor assay. It bridges current gaps between in vivo and in vitro approaches and provides a basis for a biomimetic volatile chemical sensor.

Keywords

Neuroscience; Issue 146; vapor stimulation; odorant receptors; real-time activation; odorant molecules; combinatorial code; functional assay

Correspondence to: Claire A. de March at claire.de.march@duke.edu, Hiroaki Matsunami at hiroaki.matsunami@duke.edu.

Video Link

The video component of this article can be found at https://www.jove.com/video/59446/

Disclosures

Y.F., H. K and H.M. filed a patent application relevant to this work on 27 October 2016.

Introduction

The sense of smell allows terrestrial animals to interact with their volatile chemical environment to drive behaviors and emotions. Fundamentally, the odor detection process begins with the very first interaction of odorant molecules with the olfactory system, at the level of odorant receptors (ORs)[1]. In mammals, ORs are individually expressed in olfactory sensory neurons (OSNs) located in the olfactory epithelium[2]. They belong to the G-protein coupled receptor (GPCR) family and more precisely to the rhodopsin-like sub-family (also called class A). ORs couple with the stimulatory G protein G_{olf} whose activation leads to cAMP production followed by the opening of cyclic nucleotide gated channels and the generation of action potentials. It is accepted that an odor percept relies on a specific pattern of activated ORs[3,4] and therefore odor recognition follows a combinatorial coding scheme, where one OR can be activated by a set of odorants and one odorant can activate a combination of ORs. And through such combinatorial coding, it is postulated that organisms can detect and discriminate between a myriad of volatile odor molecules. One of the keys to understanding how odors are perceived is to understand how and which ORs are activated by a given odor.

In an attempt to elucidate odorant-OR interactions, in vitro functional assays have played an essential role. The identification of agonist odorous ligands for orphan ORs (OR de-orphanization) has been a very active field for the past twenty years, through the use of various in vitro, ex vivo and in vivo functional assays[5,6,7,8,9,10,11,12,13,14,15,16,17].

In vitro assay systems are best suited for the detailed functional characterization of ORs, including identifying the functional domains and critical residues of ORs, as well as potential engineering applications. However, further development of valuable in vitro systems for ORs has been a challenge, in part due to difficulty with culturing OSNs and functional expression of ORs in heterologous cells. The first challenge had been to establish protocols that allowed for the cell surface expression of functional ORs in the mapping of odorant-OR interactions. A number of independent groups have utilized various approaches[5,6,7,8,9,10,11,12,14,18,19,20]. One of the earliest achievements was made by Krautwurst et al. in tagged the N-terminus of ORs with a shortened sequence of rhodopsin (Rho-tag) and observed an improved surface expression in human embryonic kidney (HEK) cells[13]. Variations made to the tag attached to the OR sequence is still a path explored for improving OR expression and functionality[19,21]. Saito et al. then identified receptor-transporting protein 1 (RTP1) and RTP2 which facilitate OR trafficking.[22] A shorter version of RTP1, called RTP1S, has also been shown to be even more effective than the original protein[23]. The development of a cell line (Hana3A) which stably expresses G_{olf}, REEP1, RTP1, and RTP2[24], coupled with the use of cyclic adenosine monophosphate (cAMP) reporters has enabled identification of odorant-OR interactions. The mechanism by which the RTP family of proteins promotes cell surface expression of ORs remains to be determined.

One caveat of these established methods is that they rely on odorant stimulation in liquid phase, meaning that odorants are pre-dissolved into a stimulation medium and stimulate

cells by replacing the medium. This is very distinct from the physiological conditions where odorant molecules reach the olfactory epithelium in vapor phase and activate ORs by dissolution into the nasal mucosa. To more closely resemble physiologically relevant stimulus exposure, Sanz et al.[20] proposed an assay based on vapor stimulation by applying a drop of odorant solution to hang beneath the inner face of a plastic film placed on the top of cell wells. They recorded the calcium responses by monitoring fluorescence intensity. This method was the first to use air-phase odorant stimulation, but it did not allow a large screening of OR activation.

Here, we developed a new method that enables real-time monitoring of in vitro OR activation via vapor phase odorant stimulation by the Glosensor assay (Figure 1). This assay has been used previously in the context of liquid odorant stimulation[18,19,25,26,27,28,29,30,31]. The monitoring chamber of the luminometer is first equilibrated with vaporized odorant prior to plate reading (Figure 1A). Odorant molecules are then solvated into the buffer, bathing Hana3A cells expressing the OR of interest, RTP1S and the Glosensor proteins (Figure 1B). If the odorant is an agonist of the OR, the OR will switch to an activated conformation and bind the G_{olf}, activating the adenylyl cyclase (AC), and ultimately cause cAMP levels to rise. This rising cAMP will bind to and activate the Glosensor protein to generate luminescence catalyzing luciferin. This luminescence is then recorded by the luminometer and enables OR activation monitoring. This method is of high interest in the context of OR deorphanization as it brings in vitro systems closer to the natural perception of odors.

Protocol

1. Hana3A Cells Culture

1. Prepare M10 (Minimum Essential Medium (MEM) plus 10 % v/v fetal bovine serum (FBS)) and M10PSF (M10 plus 100 µg/mL penicillin-streptomycin and 1.25 µg/mL amphotericin B).
2. Culture the cells in 10 mL of M10PSF in a 100 mm cell culture dish in an incubator set at 37 °C and 5% carbon dioxide (CO_2).
3. Divide the cells every 2 days at a 20% ratio: when 100% confluence of cells (approximately 1.1 x 10^7 cells) is observed under a phase-contrast microscope, aspire the media and wash the cells gently with 10 mL of phosphate-buffered saline (PBS).
4. Aspirate PBS and add 3 mL of 0.05% trypsin-ethylene diamine tetraacetic acid (EDTA, 0.48 mM). Let act for approximately 1 min, until the cells dissociate from the plate.
5. Add 5 mL of M10 to inactivate the trypsin and eventually detach the cells still attached to the plate by pipetting up and down.
6. Transfer the volume (8 mL) to a 15 mL tube and centrifuge at 200 x *g* for 5 min. Aspirate the supernatant and resuspend the cells into 5 mL of M10PSF by pipetting up and down to break any cell mass. Avoid creating bubbles in the tube.

7. Transfer 1 mL of the resuspended cells solution in a new 100 mm cell culture dish and add 9 mL of fresh M10PSF. Incubate at 37 °C and 5% CO_2.

2. Preparation of the Cells for Transfection

1. Evaluate the confluence, or the number of cells, by observing them under a phase-contrast microscope. At least 10% confluence (approximately 1.1 x 10^6 cells) is needed for one plate.
2. Aspirate the media and wash the cells gently with 10 mL of PBS. Aspirate PBS and add 3 mL of EDTA. Let act for approximately 1 min at room temperature, until the cells dissociate from the plate.
3. Add 5 mL of M10 to inactivate the trypsin and eventually detach the cells still attached to the plate by pipetting up and down. Transfer the volume (8 mL) to a 15 mL tube and centrifuge at 200 x *g* for 5 min.
4. Aspirate the supernatant and resuspend the cells into 5 mL of M10PSF by pipetting up and down to break any cell mass. Avoid creating bubbles in the tube.
5. Depending on the number of plates to be transfected, transfer an appropriate amount of cells in a reservoir with the proper corresponding volume of M10PSF. One 96-well plate should be plated with 1/10 of a 100% confluent 100 mm dish (approximately 1.1 x 10^6 cells) diluted in M10PSF to reach a total volume of 6 mL. For one 96-well plate starting with a 100% confluence 100 mm dish, add 500 µL from the 5 mL of resuspended cells to 5.5 mL of fresh M10PSF. Mix the cells and M10PSF without generating air bubbles.
6. Pipette 50 µL of the suspended cells into each well of the 96-well plate using a multichannel pipette. Incubate overnight at 37 °C and 5 % CO_2.

3. Plasmid Transfection

1. Observe the 96-well plate under a phase-contrast microscope to assure a cell confluence between 30% and 50%.
2. Prepare a first transfection mix that contains the plasmids common to the entire plate (RTP1S, OR and Glosensor protein, see Table of Materials) following the volumes in Table 1. Notice that the quantity of Rho-tagged OR should be divided by the number of ORs if several ORs.

   NOTE: We strongly advice to add an empty vector negative control (here Rho-pCI) and any positive control (OR known to respond to the tested odorant) to the experiment plan.
3. Prepare a second transfection mix containing 500 µL of MEM and 20 µL of Lipofectamine 2000 reagent (valid for one 96-well plate, see Table of Materials). Add the second mix to the first one, and gently mix by pipetting up and down and incubate for 15 min at room temperature. Add 5 mL of M10 and mix gently.
4. Replace the M10PSF in the previously platted 96-well plate by 50 µL of the final transfection media. Incubate in an incubator set to 37 °C and 5% CO_2 and

vacuum the chamber of the luminometer overnight following the procedure described in step 6.

4. Substrate Incubation

1. Observe the 96-well plate under a phase-contrast microscope to assure a cell confluence between 60% and 100%. Prepare a stimulation solution of Hank's Balanced Salt Solution (HBSS) containing 10 mM of hydroxyethyl piperazineethanesulfonic acid (HEPES) and 5 mM of D-glucose.
2. Dilute 75 µL of the cAMP reagent (see Table of Materials) solution to 2.75 mL of the stimulation solution. Remove the transfection medium from the 96-well plate and wash the cells by adding 50 µL of fresh stimulation solution to each well.
3. Remove the stimulation solution and add 25 µL of cAMP reagent solution prepared in step 4.2 to each well. Incubate the 96-well plate at room temperature in a dark and odor-free environment (for example, a clean empty drawer far away from chemicals or any odorant source) for 2 h.

5. Odorant Stimulation

1. First, equilibrate the luminometer chamber with volatile odorant molecules. Dilute the odorant to the desired concentration in 10 mL of mineral oil (Figure 2A). Before the end of the cAMP reagent incubation time, add 25 µL of the odorant solution in a new 96-well plate (not the one containing the cells). Incubate this odorant plate at room temperature in the luminometer chamber for 5 min (Figure 2B) (no luminometer recording is required here).
2. Set the luminometer to record the luminescence with 0 s of delay during 20 cycles of plate measurement of 90 s with 0.7 s of interval between cycles.
3. Right before reading the plate, remove the odorant plate from the chamber. Add 25 µL of odorant between the wells of the 96-well plate containing the cells (do not add the odorant in the wells containing the cells) and quickly start the luminescence measurement of all wells for 20 cycles within 30 min (Figure 2C).

6. Removal of remaining odorant inside the Luminometer

1. Open the door of the luminometer. Insert the tube connected to the vacuum pump.
2. Vacuum odorants in the reading chamber extensively (at least 2 h, preferably overnight) between two odorants to avoid cross contamination of odor volatiles from one experiment to another. Replace with fresh air by sending compressed air during 5 min before incubating the next odorant.

7. Data Analysis

1. Export the data from the luminometer software.

2. Average the replicates of the same OR for each recording time. Calculate the normalized OR response to any eventual control (e.g., Empty vector, Figure 3A and representative results section) by dividing the control averaged value to the OR averaged value at each recording time (Figure 3B and representative results section).

3. Normalize the each OR response to their basal activity by dividing the averaged OR response at 0 s to each recording time response (See Figure 3C and representative results section).

4. Calculate the area under the curve of each OR to obtain a single OR response value. To do so, sum all the luminescence values of each recording time for each OR.

Representative Results

We screened the response of three mouse ORs, Olfr746, Olfr124 and Olfr1093 using cinnamaldehyde vapor stimulation (Figure 3). Simultaneously, we used an empty vector control (Rho-pCI) to assure that the odorant-induced activities of the tested ORs were specific (Figure 3A). The real-time activation of the ORs upon vapor odorant stimulus was monitored over 20 measurement cycles. The data for each well were first normalized to the empty vector control averaged value for each cycle (Figure 3B). It is important to note that ORs can show variable levels of basal activity in this assay in an OR-dependent manner and it can be important to also normalize their response to this parameter (Figure 3C). The average value of an OR can be divided by its response at t = 0 s, allowing to compare between ORs. Single activation values for each OR can also be computed by calculating the area under the curve (AUC) for each OR by summing all measurement cycle values (Figure 3D).

Additionally, dose-dependent responses can be measured using this method using increasing odorant doses. We present the response of Olfr1377 to acetophenone stimulation recorded following the same procedure (Figure 4). Acetophenone volatility can be evaluated by its vapor pressure, which is equal to 0.44 mm Hg at 25 °C. At a given temperature, an odorant possessing a higher vapor pressure is more volatile than an odorant with a lower vapor pressure. Acetophenone is, in consequence, a moderately volatile odorant and is exposed to the cell pure and diluted at 10^{-2}, 10^{-4}, 10^{-6} and 10^{-8}. Only the three higher concentrations (pure, 10^{-2} and 10^{-4}) are able to activate Olfr1377 (Figure 4A). We can also notice that the pure compound stimulation shows a tendency to decrease the OR response during time, likely due to cell toxicity, as it has been shown for eugenol in a recent publication[32]. Nevertheless, we can observe a typical dose dependency behavior of Olfr1377 (Figure 4B), showing that this method can also be used to determine the EC50 of OR to volatile compound.

Note that when dose-dependent experiments are performed, we do not vacuum clean the luminometer chamber. However, experiments are always performed from low to high, increasing odorant doses to minimize contaminations. Further, since the real concentration of odorant molecules in the cell media is not known, the EC50s obtained by this method are

not necessarily comparable to those obtained by liquid stimulation. The EC50 values determined by our method take into account the odorant volatility, the kinetics of odorant dissolution into the medium, the odorant's solubility, and the affinity between the odorant and the OR, which are closer to the natural perception of odor. For our example of Olfr1377 stimulation by acetophenone, the EC50 value from our vapor dose-response is 161 μM (0.001874 %), which is around 50 fold higher than the liquid stimulation (3.28 μM from Saito et al.[6]). This difference between liquid and vapor stimulations was also reported by Sanz et al.[20] in their vapor stimulation assay where vapor stimulation gave 100 to 1000 fold lower EC50 values than the liquid stimulation.

Discussion

The perception of odor is fundamentally dependent on the activation of ORs. Consequently, understanding of their functionality is required to crack the complex mechanisms that the brain use to perceive its volatile chemical environment. However, the understanding of this process has been hampered by the difficulties in establishing a robust method to screen the OR repertoire for functionality against odorants in vitro. Cell surface and heterologous expression of ORs has been partially solved by the creation of tagged receptors[13,19] and by the discovery and optimization of the receptor-transporting proteins (RTPs) expressed in OSNs[22,23]. The first screening studies then appeared, bringing new insights to our understanding of OR function such as their odorant recognition pattern[6,7,26,33], activation mechanism[34,35], theoretical tridimensional structure[36,37], evolution[38,39], odor space[40,41,42], and implications in odor detection[43,44,45,46]. We believe that improving the in vitro methods could boost the deciphering of odor coding. As such, we here developed a new functional assay to allow the monitoring of OR activation by vaporized odorant molecules.

The success of this method depends on several critical steps. Although improved in the recent years, heterologous expression of some ORs remains difficult, which may influence OR responsiveness to odorant. The expression of ORs at the cell membrane can be evaluated in a parallel experiment using flow cytometry[19,24]. Notice that low levels of surface expression can still present robust responses in heterologous cell systems[35]. Another critical point is to avoid odorant contamination. Given the sensitivity of this assay, odorant molecules from any perfume, food, or previous assay can pollute the experiment by inducing uncontrolled OR responses. This is why we advise to vacuum the chamber of the luminometer for at least 2 h, preferably overnight, before performing an assay with a different odorant. It is also important to consider a potential cytotoxicity of the odorant used in the experiment. A potential decrease of the response of the OR during the 30 min monitoring can show that the odorant itself has a negative effect on the cell health. The odorant cytotoxicity can be evaluated by performing a cell viability assay after exposing the cells to the odorant. To mitigate this problem, it is possible to consider only the first 10 min of the recording time for the analysis of data, cropping the end. We noticed that odorant toxicity mainly occurs when the odorant is tested pure or at very high concentrations. The sensitivity of our assay allows the detection of odorant diluted in mineral oil. The optimal concentration to elicit maximal response varies from one odorant to another, but we observed that a 1% dilution is enough to elicit a saturation of an OR response[32]. However, some odorant molecules can possess low vapor pressure (and therefore low volatility) and

may need some adjustments to be made to the presented protocol. The incubation time of the odorant in the luminometer chamber here is set to 5 min. We assumed that this amount of time is sufficient to equilibrate the chamber with odorant volatile molecules, but low volatility odorants may require longer incubation times.

Apart from these critical points, this method brings many new possibilities to exploring the structure-function relationships of odorant-OR interactions. The real-time monitoring aspect of this method also allows for the understanding of the kinetics of events that occur during an odor perception. As an example, we used the protocol to explore the functionality of a metabolite enzyme, the carboxyl esterase 1d (Ces1d), found to be expressed in the olfactory mucosa of mammals[47]. This enzyme is known to convert esters to carboxylic acid and alcohol[48]. The co-transfection of Ces1d showed a modulation of in vitro OR responses to ester compounds,[32] demonstrating that this new protocol is efficient in exploring the importance of metabolic enzymes in odorant detection. Furthermore, using this platform to investigate odorant mixtures, and the way odors are presented in settings that are more natural, will enable future study in understanding more complex odorant interactions. Finally, detection of odorant molecules by ORs is also of high interest in the development of an odor sensor. Having shown that our system can detect odorant molecules presented in a vapor phase, this method is a first step in the development process of a miniaturized biosensor.

Acknowledgments

This work was supported by grants from NIH (DC014423 and DC016224) and the Defense Advanced Research Project Agency RealNose Project. YF stayed at Duke University with financial support from JSPS Program for Advancing Strategic International Networks to Accelerate the Circulation of Talented Researchers (R2801). We thank Sahar Kaleem for editing of the manuscript.

References

1. Buck L, Axel R A novel multigene family may encode odorant receptors: a molecular basis for odor recognition. Cell. 65 (1), 175–187 (1991). [PubMed: 1840504]
2. Serizawa S, Miyamichi K, Sakano H One neuron–one receptor rule in the mouse olfactory system. Trends in Genetics. 20 (12), 648–653 (2004). [PubMed: 15522461]
3. Malnic B, Hirono J, Sato T, Buck LB Combinatorial receptor codes for odors. Cell. 96 (5), 713–723 (1999). [PubMed: 10089886]
4. Hallem EA, Carlson JR Coding of odors by a receptor repertoire. Cell. 125 (1), 143–160 (2006). [PubMed: 16615896]
5. Peterlin Z, Firestein S, Rogers ME The state of the art of odorant receptor deorphanization: a report from the orphanage. The Journal of General Physiology. 143 (5), 527–542 (2014). [PubMed: 24733839]
6. Saito H, Chi Q, Zhuang H, Matsunami H, Mainland JD Odor coding by a Mammalian receptor repertoire. Science Signal. 2 (60), ra9–ra9 (2009).
7. Geithe C, Noe F, Kreissl J, Krautwurst D The broadly tuned odorant receptor OR1A1 is highly selective for 3-methyl-2, 4-nonanedione, a key food odorant in aged wines, tea, and other foods. Chemical Senses. 42 (3), 181–193 (2017). [PubMed: 27916747]
8. Nishizumi H, Sakano H Decoding and deorphanizing an olfactory map. Nature Neuroscience. 18 (10), 1432 (2015). [PubMed: 26404718]
9. Wetzel CH et al. Functional expression and characterization of a Drosophila odorant receptor in a heterologous cell system. Proceedings of the National Academy of Sciences. 98 (16), 9377–9380 (2001).

10. Touhara K et al. Functional identification and reconstitution of an odorant receptor in single olfactory neurons. Proceedings of the National Academy of Sciences. 96 (7), 4040–4045 (1999).
11. Levasseur G et al. Ligand#specific dose–response of heterologously expressed olfactory receptors. European Journal Of Biochemistry. 270 (13), 2905–2912 (2003). [PubMed: 12823561]
12. Zhao H et al. Functional expression of a mammalian odorant receptor. Science. 279 (5348), 237–242 (1998). [PubMed: 9422698]
13. Krautwurst D, Yau K-W, Reed RR Identification of ligands for olfactory receptors by functional expression of a receptor library. Cell. 95 (7), 917–926 (1998). [PubMed: 9875846]
14. Wetzel CH et al. Specificity and Sensitivity of a Human Olfactory Receptor Functionally Expressed in Human Embryonic Kidney 293 Cells andXenopus Laevis Oocytes. Journal of Neuroscience. 19 (17), 7426–7433 (1999). [PubMed: 10460249]
15. Kajiya K et al. Molecular bases of odor discrimination: reconstitution of olfactory receptors that recognize overlapping sets of odorants. Journal of Neuroscience. 21 (16), 6018–6025 (2001). [PubMed: 11487625]
16. Jiang Y et al. Molecular profiling of activated olfactory neurons identifies odorant receptors for odors in vivo. Nature Neuroscience. 18 (10), 1446 (2015). [PubMed: 26322927]
17. Von Der Weid B et al. Large-scale transcriptional profiling of chemosensory neurons identifies receptor-ligand pairs in vivo. Nature Neuroscience. 18 (10), 1455 (2015). [PubMed: 26322926]
18. Geithe C, Andersen G, Malki A, Krautwurst D A butter aroma recombinate activates human class-I odorant receptors. Journal of Agricultural and Food Chemistry. 63 (43), 9410–9420 (2015). [PubMed: 26451762]
19. Noe F et al. IL-6–HaloTag® enables live-cell plasma membrane staining, flow cytometry, functional expression, and de-orphaning of recombinant odorant receptors. Journal of Biological Methods. 4 (4), e81 (2017). [PubMed: 31453235]
20. Sanz G, Schlegel C, Pernollet J-C, Briand L Comparison of odorant specificity of two human olfactory receptors from different phylogenetic classes and evidence for antagonism. Chemical Senses. 30 (1), 69–80 (2005). [PubMed: 15647465]
21. Shepard BD, Natarajan N, Protzko RJ, Acres OW, Pluznick JL A cleavable N-terminal signal peptide promotes widespread olfactory receptor surface expression in HEK293T cells. PLoS One. 8 (7), e68758 (2013). [PubMed: 23840901]
22. Saito H, Kubota M, Roberts RW, Chi Q, Matsunami H RTP family members induce functional expression of mammalian odorant receptors. Cell. 119 (5), 679–691 (2004). [PubMed: 15550249]
23. Wu L, Pan Y, Chen G-Q, Matsunami H, Zhuang H Receptor-Transporting Protein 1 Short (RTP1S) Mediates the Translocation and Activation of Odorant Receptors by Acting through Multiple Steps. Journal of Biological Chemistry. jbc. M112. 345884 (2012).
24. Zhuang H, Matsunami H Evaluating cell-surface expression and measuring activation of mammalian odorant receptors in heterologous cells. Nature Protocols. 3 (9), 1402 (2008). [PubMed: 18772867]
25. Zhang Y, Pan Y, Matsunami H, Zhuang H Live-cell Measurement of Odorant Receptor Activation Using a Real-time cAMP Assay. Journal of Visualized Experiments. (128), e55831–e55831 (2017).
26. Li S et al. Smelling sulfur: Copper and silver regulate the response of human odorant receptor OR2T11 to low-molecular-weight thiols. Journal of the American Chemical Society. 138 (40), 13281–13288 (2016). [PubMed: 27659093]
27. Ahmed L et al. Molecular mechanism of activation of human musk receptors OR5AN1 and OR1A1 by (R)-muscone and diverse other musk-smelling compounds. Proceedings of the National Academy of Sciences. 115 (17), E3950–E3958 (2018).
28. Duan X et al. Crucial role of copper in detection of metal-coordinating odorants. Proceedings of the National Academy of Sciences. 109 (9), 3492–3497 (2012).
29. Sekharan S et al. QM/MM model of the mouse olfactory receptor MOR244–3 validated by site-directed mutagenesis experiments. Biophysical journal. 107 (5), L5–L8 (2014). [PubMed: 25185561]
30. Liu MT et al. Carbon chain shape selectivity by the mouse olfactory receptor OR-I7. Organic & Biomolecular Chemistry. 16 (14), 2541–2548 (2018). [PubMed: 29569669]

31. Li Y et al. Aldehyde Recognition and Discrimination by Mammalian Odorant Receptors via Functional Group-Specific Hydration Chemistry. ACS Chemical Biology. 9 (11), 2563–2571 (2014). [PubMed: 25181321]
32. Kida H et al. Vapor detection and discrimination with a panel of odorant receptors. Nature Communications. 9 (1), 4556 (2018).
33. Yu Y et al. Responsiveness of G protein-coupled odorant receptors is partially attributed to the activation mechanism. Proceedings of the National Academy of Sciences. 112 (48), 14966–14971 (2015).
34. de March CA et al. Conserved residues control Activation of mammalian G protein-coupled odorant receptors. Journal of the American Chemical Society. 137 (26), 8611–8616 (2015). [PubMed: 26090619]
35. de March CA et al. Odorant receptor 7D4 activation dynamics. Angewandte Chemie. 130 (17), 4644–4648 (2018).
36. Kim S-K, Goddard WA Predicted 3D structures of olfactory receptors with details of odorant binding to OR1G1. Journal of Computer-Aided Molecular Design. 28 (12), 1175–1190 (2014). [PubMed: 25224127]
37. de March CA, Kim SK, Antonczak S, Goddard WA III, Golebiowski J G protein#coupled odorant receptors: From sequence to structure. Protein Science. 24 (9), 1543–1548 (2015). [PubMed: 26044705]
38. Adipietro KA, Mainland JD, Matsunami H Functional evolution of mammalian odorant receptors. PLoS Genetics. 8 (7), e1002821 (2012). [PubMed: 22807691]
39. Mainland JD et al. The missense of smell: functional variability in the human odorant receptor repertoire. Nature Neuroscience. 17 (1), 114 (2014). [PubMed: 24316890]
40. Meister M On the dimensionality of odor space. Elife. 4 e07865 (2015). [PubMed: 26151672]
41. Bushdid C, Magnasco MO, Vosshall LB, Keller A Humans can discriminate more than 1 trillion olfactory stimuli. Science. 343 (6177), 1370–1372 (2014). [PubMed: 24653035]
42. Gerkin RC, Castro JB The number of olfactory stimuli that humans can discriminate is still unknown. Elife. 4 e08127 (2015). [PubMed: 26151673]
43. Shirasu M et al. Olfactory receptor and neural pathway responsible for highly selective sensing of musk odors. Neuron. 81 (1), 165–178 (2014). [PubMed: 24361078]
44. Keller A, Zhuang H, Chi Q, Vosshall LB, Matsunami H Genetic variation in a human odorant receptor alters odour perception. Nature. 449 (7161), 468 (2007). [PubMed: 17873857]
45. McRae JF et al. Genetic variation in the odorant receptor OR2J3 is associated with the ability to detect the “grassy” smelling odor, cis-3-hexen-1-ol. Chemical Senses. 37 (7), 585–593 (2012). [PubMed: 22714804]
46. de March CA, Ryu S, Sicard G, Moon C, Golebiowski J Structure–odour relationships reviewed in the postgenomic era. Flavour and Fragrance Journal. 30 (5), 342–361 (2015).
47. Olson MJ, Martin JL, LaRosa AC, Brady AN, Pohl LR Immunohistochemical localization of carboxylesterase in the nasal mucosa of rats. Journal of Histochemistry & Cytochemistry. 41 (2), 307–311 (1993). [PubMed: 8419465]
48. Nagashima A, Touhara K Enzymatic conversion of odorants in nasal mucus affects olfactory glomerular activation patterns and odor perception. Journal of Neuroscience. 30 (48), 16391–16398 (2010). [PubMed: 21123585]

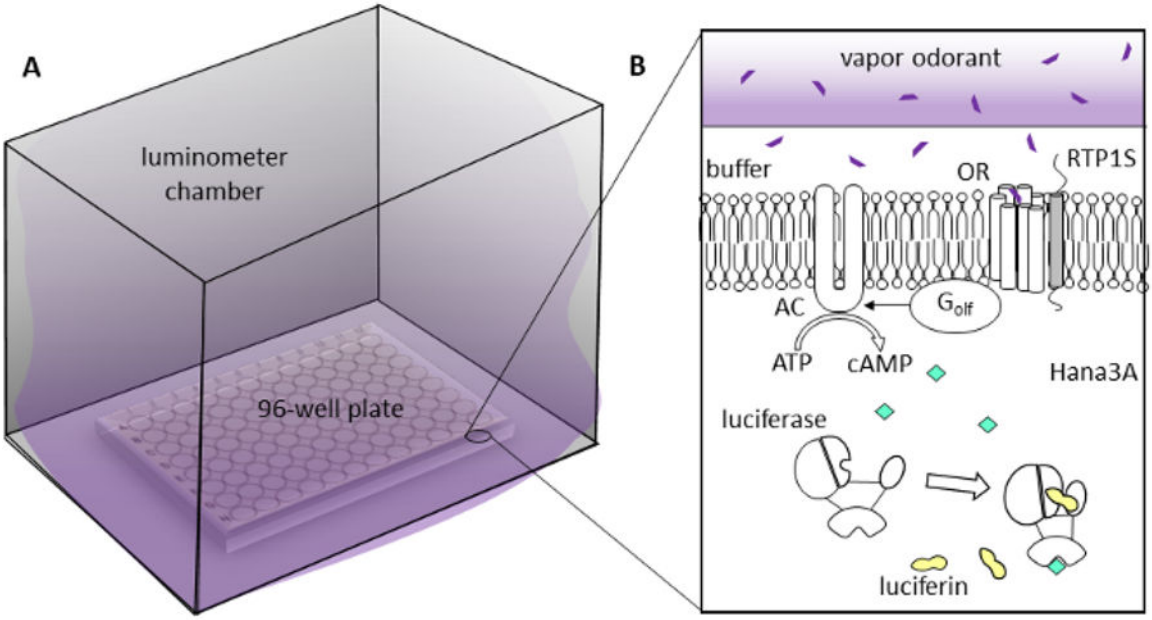

Figure 1: Principle of real-time monitoring of odorant receptor activation by vapored odorant.

(**A**) The 96-well plate was placed into the already equilibrated with odor (violet cloud) luminometer chamber. (**B**) Vaporized odorant molecules (violet) at the surface of the cell media buffer dissolved into it to reach the OR cavity, at the Hana3A cell membrane surface. The accessory protein RTP1S (gray) was transfected as well, to favor the cell surface expression of the OR. If the odorant molecule was an OR agonist, the OR switched to an activated state and bound the G_{olf}, triggering the activation of adenylyl cyclase (AC) and the production of cyclic AMP (cAMP; green). The Glosensor protein (luciferase) possesses a binding site for cAMP that, once bound, allows the protein to bind its ligand, the luciferin (yellow). The final complex Glosensor protein/luciferin/cAMP produced the luminescence that was recorded to monitor the OR activation.

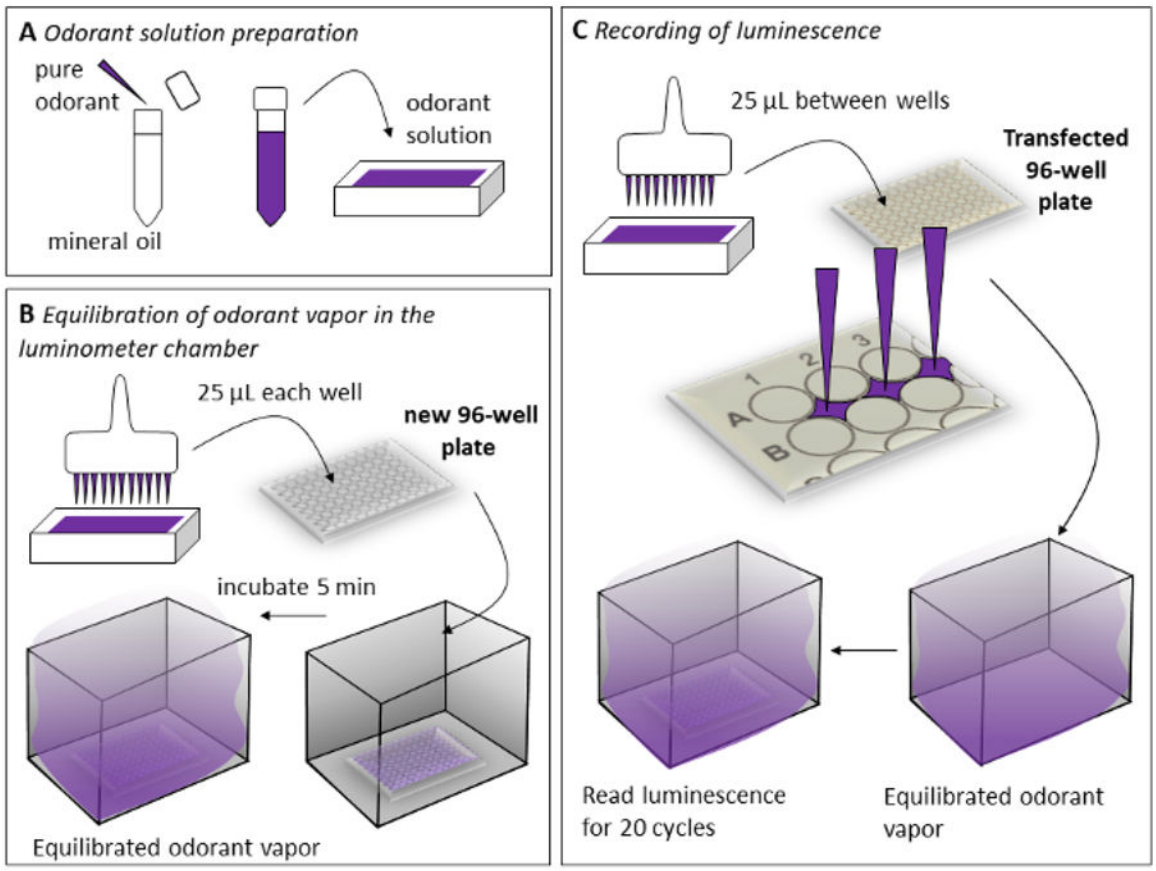

Figure 2: Schematic protocols for real-time monitoring of odorant receptor activation by vapored odorant.

The odorant (violet) was diluted at the desired concentration in mineral oil (**A**). The solution was then plated into a new 96-well plate, which was placed into the luminometer chamber for 5 min to equilibrate the volume with vapored odorant before monitoring the transfected 96-well plate (**B**). The odorant solution was pipetted into each space between the wells of the transfected 96-well plate (see zoom). The plate was then read for 20 cycles in the luminometer chamber equilibrated vapor odorant (**C**).

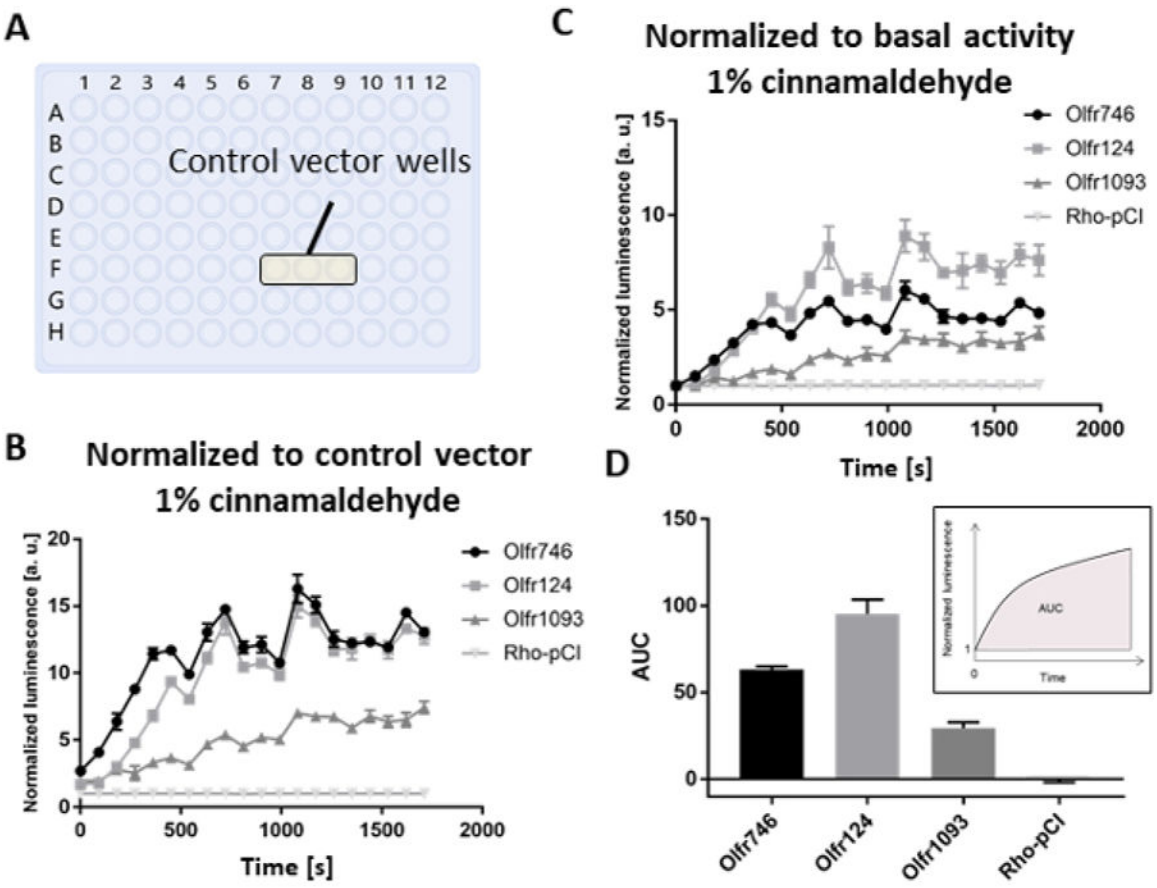

Figure 3: Example of normalization that can be performed after data recording.

(**A**) An empty vector (negative) control was inserted in the transfection plan to be able to identify any potential non-OR specific odor activations of cells. It also provided information on the background luminescence of the plate. **(B**) Each OR response was then normalized by dividing the emission value of each well by the average value of the control vector in each plate. The luminescence values of each OR were then averaged along the measurement cycles. (**C**) OR responses can also then be normalized to their basal activity by further dividing each cycle value by the average value of the 1st cycle of measurement (t = 0 s). (**D**) The AUC can be calculated by summing the emission values of each measurement cycle. For B, C and D, error bars represent the standard error of the mean (SEM, n = 3).

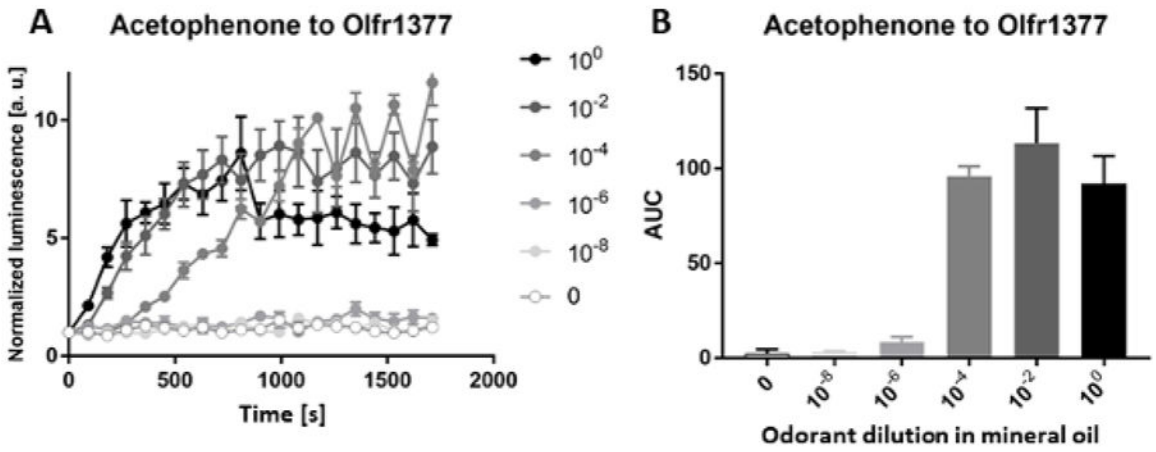

Figure 4. Example of dose dependent responses obtained with the method.

(**A**) The response of Olfr1377 to acetophenone was recorded for five different dilutions in mineral oil (10^0, 10^{-2}, 10^{-4}, 10^{-6}, 10^{-8}), and without odorant (0), and normalized following the normalization protocol shown in Figure 3. (**B**) The data during the measurement cycles was translated into an AUC value for each dilution. This figure has been modified from Kida et al.[32]. This figure is licensed under a Creative Commons Attribution 4.0 International (CC BY 4.0). Error bars represent the standard error of the mean (SEM, n = 3).

Table 1:

Mix for transfection.

	Per 96-well plate
MEM	500 μL
pGlosensor	10 ng
RTP1S	5 ng
OR	75 ng

Quantities of plasmids (Glosensor protein, RTP1S and OR) to add to MEM to transfect to one 96-well plate.

Table of Materials

Name of Material/Equipment	Company	Catalog Number	Comments/Description
0.05 % trypsin-EDTA	Gibco	25300-054	0.05% Trypsin - EDTA (1x), phenol red - store at 4°C
100 mm cell culture dish	BD Falcon	353003	100 mm x 20 mm cell culture dish
15 mL tube	BD Falcon	352099	17 mm x 120 mm conical tubes
96-well plate	Corning	3843	96 well, with LE lid white with clear bottom Poly-D-lysine coated Polystyrene
Amphotericin	Gibco	15290-018	Amphotericin B 250 µg/mL - store at 4°C
centrifuge machine	Jouan	C312	Centrifuge machine with swinging bucket rotor for 15 mL
Class II Type A/B3 fumehood	NUAIRE	NU-407-500	fumehood for cell culturing
FBS	Gibco	16000-044	Fetal Bovine Serum - store at −20°C
GloSensor cAMP Reagent	Promega	E1290	GloSensor cAMP Reagent luminescent protein substrate - store at −20°C
Incubator 37 °C; 5 % CO_2	Fisher Scientific	11-676-604	Incubator for cell culturing
Lipofectamine 2000 reagent	Invitrogen	11668-019	Lipofectamine 2000 Reagent 1mg/ml transfection reagent - store at 4°C
Luminometer POLARstar OPTIMA	BMG LABTECH	discontinued	96 well plate reader for luminescence
Mineral oil	Sigma	M8410	Solvent for odorants - store at room temperature
Minimum Essential Medium (MEM)	Corning cellgro	10-010-CV	Minimum Essential Medium Eagle with Earle’s salts & L-glutamine - store at 4°C
Penicillin/Streptomycin	Sigma Aldrich	P4333	Penicillin-Streptomycin solution stabilized with 10,000 U of penicillin and 10 mg streptomycin - store at −20°C
pGlosensor	Promega	E2301	pGloSensor-22F cAMP luminescent protein plasmid - store at 4°C
phase contrast microscope	Leica	090-131.001	phase contrast microscope with x4, x10, x20 objectives
RTP1S	H. Matsunami lab	-	100 ng/µL plasmid - store at 4°C